Introduction to the Combined Finite–Discrete Element Method

Máté Hazay
Budapest University of Technology and Economics, Hungary

Ante Munjiza
Queen Mary University of London, England

ABSTRACT

This chapter presents a general overview of the combined finite-discrete element method (FEM/DEM) which is considered as a state-of-the-art technique for the mechanical analysis of masonry structures. In a FEM/DEM simulation each discrete element representing a stone block is discretised into finite elements in order to describe the deformability of the blocks. This chapter deals with the main steps of the FEM/DEM including contact detection, contact interaction, fracture and fragmentation algorithms, calculation of deformations and the time integration of the equation of motion. The FEM/DEM is advantageously used to simulate transition from continua to discontinua processes which may lead to the collapse of the structure. Some examples for practical applications found in the literature are mentioned.

Keywords: Contact detection, Contact interaction, Potential force concept, Green-St. Venant tensor, Fracture, Fragmentation, Central difference method, Parallelization, Ante Munjiza, Y3D

INTRODUCTION

The two basic types of mechanical models are the classical models of continuum mechanics and the models of discrete elements. The *finite element method* (*FEM*) is the most widely used technique to model continuum mechanical problems. On the other hand, the *discrete element method* (*DEM*) is able to describe discontinuum-based phenomena including the motion and interaction of individual particles. However in certain situations the two different phenomena arise at the same time, thus the development of a coupled numerical tool was required. Therefore, in the early 1990s the two above mentioned methods have been combined and the resulting method was termed the *combined finite-discrete element method (FEM/DEM)*. A typical *combined finite-discrete element* simulation comprises large number – thousands or even millions – of particles which are represented by a single discrete element. In *FEM/DEM e*ach discrete element is discretized into finite elements in order to describe the deformations of the blocks. Furthermore, the classical steps of *discrete element method*, including contact detection, contact interaction and time integration are applied to follow the motion and interaction of the individual particles. This method was implemented mainly to simulate so-called *transition from continua to discontinua* problems, including failure, fracture and fragmentation processes. Thus, detailed structural collapse simulations can be performed with the help of the *FEM/DEM*. These simulations can play a vital role in the design of structures against hazardous loading conditions. In this case the load bearing capacity of the structure can be determined, and the progressive collapse modes can be identified as well. Some examples for modelling *transition from continua to discontinua* problems can be found in (Munjiza, 2004, pp. 30-32).

The *combined finite discrete element method* can be an advantageous tool for modelling of masonry structures. Masonry is a heterogeneous structural material consisting of bricks joined by mortar layers. The numerical modelling of masonry structures - especially in the nonlinear range - represents an interesting challenge due to the extremely complex behaviour deriving from their semi-discrete, composite nature. Two different approaches exist for mechanical modelling of masonry structures, these are the micro modelling and macro modelling of masonry structures. In case of macro modelling approach, the structure is handled as an orthotropic continuum and the constitutive relations are described with the help of experiments and homogenization techniques. The serious disadvantage of this continuum-based approach is its inability to describe large discontinuities which occur during the collapse process. In order to ease this restriction contact elements may be implemented into the finite element mesh. This approach enables to consider the material nonlinearity where the constitutive behaviour of the contact elements are prescribed according to the theory of plasticity or damage mechanics. Unfortunately, even with the application of contact elements, the *finite element method* is unable to handle the mechanical interaction of several blocks. Due to this fact reliable collapse simulations including progressive failure modes cannot be carried out with the application of the *FEM*. However numerical models based on the *combined finite-discrete element method* have been developed for the analysis of such problems where the mechanical interaction between several deformable bodies must be followed. The *FEM/DEM* uses this previously mentioned joint element approach to describe the fracturing behaviour of an initially continuum-like solid block represented by a single discrete element. Therefore, in *combined finite-discrete element* simulations the number of discrete elements may vary during the collapse process. Since *FEM/DEM* includes contact detection and contact interaction algorithms, this technique is capable of modelling the mechanical interaction of several bodies.

The appropriate computational modelling of the response of masonry structures must involve all of the fundamental mechanisms which affect the failure process, like the sliding and splitting of the blocks along the mortar joints and cracking of the individual units under certain stress conditions. The *combined finite-discrete element* method proved to be a very effective tool for the analyses of the non-linear behaviour of masonry structures. The advantage of this method derives from the possibility to model the whole process of the structural response starting from the linear-elastic phase, followed by the non-linear range comprises crack initiation, crack propagation, and sliding effects. The motion and interaction of the particles are followed considering inertia effects until the final, state of rest situation is reached due to the energy dissipation of the structure. The *FEM/DEM* can be a very advantageous technique, particularly in case of cyclic loading situations, where the appropriate modelling of the creation of new contacts due to the redistribution of the system topology is a fundamental demand. At the end of this chapter several examples for analyses of structural response under cyclic loading conditions are mentioned.

In the following sub-chapters the main processes of the *combined finite-discrete element method* are mentioned including contact detection, contact interaction, fracture and fragmentation algorithms, calculation of deformations, parallelization and the time integration of the equations of motion. Different modelling approaches and examples connected to the structural analysis of masonry structures are mentioned found in the literature.

BASIC CHARACTERISTICS OF THE MECHANICAL MODEL

This sub-chapter focuses on the basic characteristics of the mechanical model considered in a *combined finite-discrete element* simulation. In general, a *FEM/DEM* simulation may comprise a large number of arbitrary shaped deformable discrete elements. Each discrete element represents a

continuum, thus the deformations of the solid blocks are followed by classical continuum mechanical description (i.e. each material point has translational freedoms). Since the *finite element method* is applied to follow the continuum-like behaviour, each discrete element is discretised into finite elements (mentioning that usually constant strain triangle or tetrahedron elements are used). Therefore, the shape of discrete elements and their position in space at any time instance are given by the current coordinates of the finite element nodes:

$$\boldsymbol{x} = \begin{bmatrix} x_1 \\ x_2 \\ x_3 \\ \dots \\ x_i \\ \dots \\ x_n \end{bmatrix}, \tag{1}$$

where n is the total number of degrees of freedom for a particular element. It means that *n* (i.e. the total number of the components of vector $\boldsymbol{x}$ equals the product of the number of finite element nodes and the number of translational freedoms corresponding to the nodes. Stresses can be calculated in a typical continuum mechanical approach, by using strain tensor and some kind of constitutive equation. During the calculation of the strains, usually small strains but large displacements and large rotations must be considered. After evaluating the stress field, the $\boldsymbol{F_{int}}$ vector of internal forces can be compiled by reducing the distributed internal forces to the finite element nodes following the finite element discretization. The velocity and acceleration fields over the discrete elements are described by nodal velocities $\boldsymbol{v}$ and nodal accelerations $\boldsymbol{a}$ given by:

$$\boldsymbol{v} = \dot{\boldsymbol{x}} = \begin{bmatrix} \dot{x}_1 \\ \dot{x}_2 \\ \dot{x}_3 \\ \dots \\ \dot{x}_i \\ \dots \\ \dot{x}_n \end{bmatrix}, \qquad \boldsymbol{a} = \dot{\boldsymbol{v}} = \ddot{\boldsymbol{x}} = \begin{bmatrix} \ddot{x}_1 \\ \ddot{x}_2 \\ \ddot{x}_3 \\ \dots \\ \ddot{x}_i \\ \dots \\ \ddot{x}_n \end{bmatrix}. \tag{2}$$

The interaction of neighbouring discrete elements is described by the contact detection and contact interaction algorithms. As a result of the mechanical interaction contact forces are evaluated between discrete elements. These contact forces can be assembled in $\boldsymbol{F_{ext}}$ vector of external forces, which also includes the external forces acting on discrete elements directly. Again, the number of components of this vector equals *n*, therefore concentrated forces may act at finite element nodes in the direction of each degree of freedom. Additionally, the *combined finite-discrete element method* has the speciality that discrete elements can fracture and fragment, thus the number of discrete elements comprising problem may vary during the analysis. This fracturing behaviour is described by joint elements implemented into the finite element mesh. The mechanical behaviour of these joint elements is defined by the fracture and fragmentation algorithm. The forces transmitted through joint elements can be assembled in $\boldsymbol{F_{joint}}$ vector.

The applied mechanical model may include any kind of external or internal damping effects considering in damping matrix $\boldsymbol{C}$. Additionally, since the transient dynamic motion of discrete elements are analyzed, the equation of motion must include the inertia forces as well. Due to the finite element discretization the mass is also discretized. To reduce the computational challenge the most convenient way to discretize the mass is the so-called lumped mass approach. Here it is assumed the

mass is lumped into the nodes of the finite element mesh. Thus, the mass associated with each degree of freedom is given by:

$$\boldsymbol{m} = \begin{bmatrix} m_1 \\ m_2 \\ m_3 \\ \dots \\ m_i \\ \dots \\ m_n \end{bmatrix}. \tag{3}$$

When *combined finite-discrete element* simulations comprise thousands or millions of discrete elements, then thousands or millions of separate finite element meshes are included as well. Referring to the computational challenge associated with large scale *FEM/DEM* problems, no stiffness matrices are calculated, and an explicit time integration scheme is applied on element-by-element, node-by-node and degree of freedom by degree of freedom.

Therefore, the equation of motion resulted in the following form - Eq. (4) - is solved for each element separately:

$$\boldsymbol{Ma} + \boldsymbol{Cv} + \boldsymbol{F}_{int} - \boldsymbol{F}_{ext} - \boldsymbol{F}_{joint} = \boldsymbol{0}\,. \tag{4}$$

Then, at each time step the following calculation steps are performed:

(1) Evaluation of internal forces based on deformation of particles,
(2) Evaluation of joint forces based on the deformation of joint elements,
(3) Fracture of joints,
(4) Contact detection,
(5) Contact interaction (i.e. evaluation of contact forces),
(6) Application of external forces,
(7) Solution of the equation of motion for each discrete element separately.

After the discussion of the basic characteristics of the applied mechanical model, the further sub-chapters deal with most important steps of a *FEM/DEM* simulation in a more detailed way. Firstly, the main aspects of the applied contact detection algorithms are considered.

CONTACT DETECTION ALGORITHM

In case of a *combined finite-discrete element* analysis, the transient dynamics of a large number of deformable discrete elements are simulated. One of the key issues in the development of a *FEM/DEM* code is the realistic and efficient handling of mechanical contacts formed between the discrete elements. The treatment how the mechanical behaviour of contacts are simulated is based on the contact detection and contact interaction algorithms.

In general, processing contact interaction of all possible contacts would involve a total number of computational operations proportional to the squared of the total number of discrete elements comprising the problem. In case of large-scale *FEM/DEM* simulations this would represent a huge - probably unsolvable - computational challenge, and would limit the application possibilities of *FEM/DEM* to the simulation of relatively small problems. Therefore, the main goal of contact detection algorithms is to reduce the CPU requirements of processing contact interaction, while contact detection itself must demand as small RAM and CPU requirements as possible. Contact detection algorithms reduce CPU requirements via two main steps, namely these have to eliminate

those couples that are far from each other and are surely not in contact and these have to detect all couples of discrete elements that are actually in contact. In case of a contact detection algorithm the CPU-, RAM efficiency and its easy implementation are the most important requirements beside its robustness.

Emphasizing the importance of CPU efficiency, contact detection algorithms can be classified according to the proportion how the CPU time depends on the size of the problem. Generally speaking, classical contact detection algorithms of *discrete element method* (for instance the *body-based search* technique) belong to the group of Hyper-linear contact detection algorithms meaning that the necessary CPU time increase faster than the size of the problem (i.e. number of discrete elements). Nowadays linear contact detection algorithms are used in *combined finite discrete element* simulations meaning that the CPU time is a linear function of the number of discrete elements comprising the problem. The first such an algorithm was implemented in (Munjiza, Owen, & Bicanic, 1995) and called *Munjiza-NBS contact detection algorithm*.

The *NBS contact detection algorithm* is based on space decomposition, where the space is subdivided into identical square cells as it is shown in Figure (1).

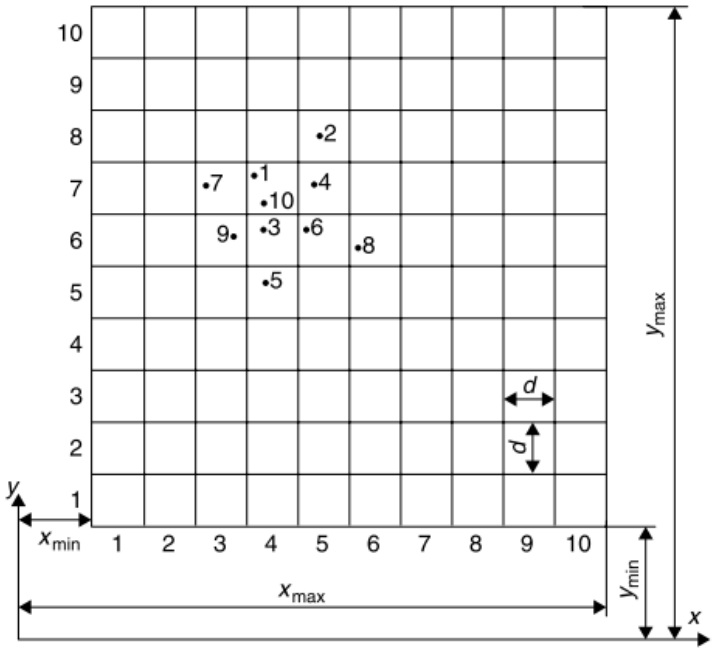

Figure 1. Space decomposition in Munjiza-NBS contact detection algorithm. Source: Munjiza, 2004

Discrete elements are assigned an integer identification number and similarly each cell is assigned an identification couple of integer numbers. Afterwards each discrete element is mapped onto cells, meaning each element is assigned to one and only one cell. Additionally, mapping of discrete elements onto columns and rows are performed. A discrete element is said to be mapped to a particular row/column of cells if it is mapped to any cell from that row/column. The CPU and RAM efficiency of *Munjiza-NBS contact detection algorithm* derives mainly from the way how it represents the mapping between discrete elements and cells, namely singly connected linked lists are used here. The representation of mapping is performed in two stages, starting with mapping of all discrete elements onto the rows of cells, and a singly connected list is formed for each row as it is shown in Figure (2).

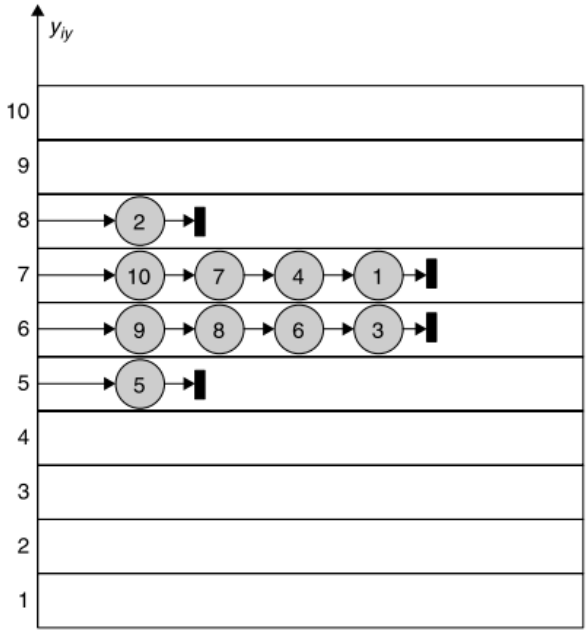

Figure 2. Singly connected lists for rows of cells. Source: Munjiza, 2004

We note that the digital representation of each list are achieved through two integer arrays. Further details can be found in (Munjiza, 2004, pp. 73-129). In the second stage, the mapping of discrete elements to individual cells are performed. After the elements were mapped onto cells, the contact detection is accomplished by checking all the discrete elements mapped to a particular cell against all discrete elements in neighbouring cells. It is important that only discrete elements from neighbouring cells can touch each other, thus for each element it is enough to check against discrete elements belonging to neighbouring - non-empty - cells. The contact detection is performed by employing a loop over discrete elements. Number of operations carried out inside the loops do not depend upon the number of discrete elements, therefore the total CPU time taken to detect all the contact is proportional to the total number of discrete elements. In the *Munjiza-NBS contact detection algorithm* no loop over cells is involved, which causes that the total CPU time is independent of the total number of cells. It means that the necessary CPU time does not depend either on the size of the finite space where the discrete elements are distributed or on the packing density. We mention that *Munjiza-NBS contact detection algorithm* can be generalized to 3D space as well. This step requires the mapping of all discrete elements onto layers of cells in *z*-direction too.

It should be mentioned that even though the contact detection operations could be done in each time step, it would be very expensive for CPU time point of view. Therefore, a so-called buffer can be introduced. The frequency of contact detection analyses can be controlled through the size of the buffer, since the contact detection process is performed only if the maximum travelled distance exceeds the size of this buffer.

Nowadays a whole range of contact detection algorithms is available for large scale *combined finite-discrete element* simulation. In general, there is not an exact answer to which is the best contact detection algorithms, hence further consideration about the selection of the applied contact detection algorithm may be necessary. The *screening array based contact detection algorithm* is one of the most efficient algorithm from CPU time point of view, however it demands enormous RAM requirements. The *sorting contact detection algorithm* is very efficient in terms of RAM requirements, but this algorithm belongs to the group of hyper-linear contact detection algorithms, meaning that for very large scale problems CPU times may be prohibitive. In terms of CPU requirements, the *Munjiza-NBS*

contact detection algorithm is more efficient than the *binary search based contact detection algorithms* or the *sorting contact detection algorithms*. Although, it uses less RAM space than the *binary search based algorithm*, the *sorting contact detection algorithms* are a little bit more efficient in terms of RAM requirements. We note that the *Munjiza-NBS contact detection algorithm* and the *sorting contact detection algorithms* have RAM requirements proportional to the number of discrete elements. Eventually, the author mention that some further effective and new contact detection algorithm can be found in the literature, referring to papers (Munjiza, Rougier, & John, 2006) and (Schiava D'Albano, Munjiza, & Lukas, 2013).

CONTACT INTERACTION ALGORITHMS

As it has been mentioned earlier, in case of *combined finite-discrete element* simulations it is absolutely essential to have an efficient and robust algorithm for handling mechanical contacts. Once elements in contact are detected due to the applied contact detection algorithm, a contact interaction algorithm is employed to evaluate the contact forces. Therefore, contact interaction is the mathematical model to compute the penetration of a discrete element into another discrete element. After calculating the penetration, contact forces are evaluated using certain constitutive relations. In case of *FEM/DEM* applications the treatment of contact interaction has a special importance. Since a *combined finite-discrete element* simulation may contain millions of deformable separate bodies which can fracture and fragment, the topology and even the size of the problem change continuously, thus handling of contacts defines the constitutive behaviour of the system. Therefore, special attention must be paid on contact kinematics and robustness in order to obtain realistic distribution of contact forces and energy balance.

In case of algorithms based on so-called *concept of the contact element* described in (Munjiza, Owen, & Bicanic, 1995) these requirements are not satisfied entirely. When the overlap of discrete elements in contact exceeds the contact layer, the energy balance is not preserved and the same is true when new surfaces are created due to fracture and fragmentation processes. Furthermore, in this concept concentrated contact forces are considered, which causes stress and strain concentrations near the boundary of elements. These stress concentrations may result in significantly unrealistic fracture and fragmentation behaviour especially in case of brittle materials.

Recognizing these phenomena the so-called *potential field-based penalty function method* was introduced (Munjiza & Andrews, 2000). Here the basic assumption is that when two bodies in contact penetrate each other, this penetration results in a contact force. For further calculations, a standard contact functional was implemented in the following way:

$$U_c = \int_\Gamma \frac{1}{2} p(\boldsymbol{r_t} - \boldsymbol{r_c})^T (\boldsymbol{r_t} - \boldsymbol{r_c})\, d\Gamma\,, \tag{5}$$

where p is the penalty term while r_t and r_c are position vectors of the points on the overlapping boundaries of the target and contactor bodies, respectively. In case of infinite penalty terms no penetration would occur, however large penalty term may cause numerical problems, thus in practical applications the *penalty function method* usually works with overlaps between discrete elements in contact. In this *potential contact force concept* distributed contact forces are considered which are evaluated from the shape and the size of overlap between the so-called contactor and target elements which form the contact. It is assumed that in the situation of elementary penetration where the overlapping area is dA, an infinitesimal contact force arises given by:

$$d\boldsymbol{f} = [grad\varphi_c(P_c) - grad\varphi_t(P_t)]dA = d\boldsymbol{f_c} - d\boldsymbol{f_t} \tag{6}$$

where $d\boldsymbol{f}$ is the infinitesimal contact force, due to the overlap dA defined by overlapping points P_c - belonging to the contactor - and P_t - belonging to the target. As it is shown in Eq. (6), the contact can be viewed firstly as the elemental area of the contactor penetrating the target and then the elemental area of the target penetrating the contactor. The previous formula also shows that the contact force can be calculated as the gradient of the corresponding potential function, thus contact forces form a conservative vector field. Due to this fact, if point P_c of the contactor element penetrates the target through any path defined by end point A and B, the total work of the contact force does not depend on path but on the end points only and it is given as $\varphi_t(A) - \varphi_t(B)$.

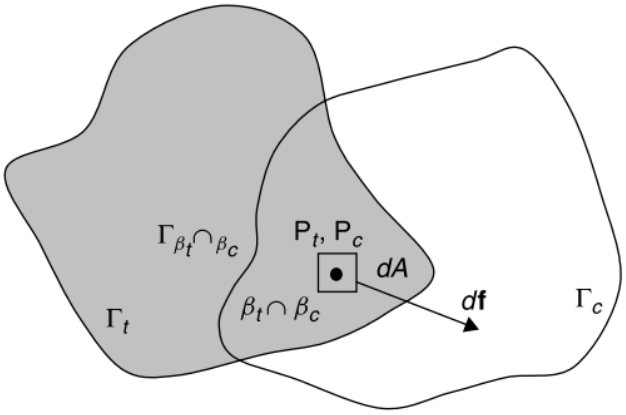

Figure 3 Contact force due to an infinitesimal overlap around points $\boldsymbol{P_c}$ and $\boldsymbol{P_t}$
Source: Munjiza, 2004

An important aspect is that when point A and B are placed on the boundary of the target discrete element, a contact-contact release situation arises, when the energy preservation law requires that no work is done by the contact force, ie.:

$$\varphi_t(A) - \varphi_t(B) = 0 \; and \; \varphi_c(A) - \varphi_c(B) = 0\,. \tag{7}$$

Therefore, if Eq. (7) is valid for every arbitrary boundary points of the contactor and target elements, then the contact force given by Eq. (6) preserves the energy balance regardless of the geometry or the shape of the contacting elements, the size of the overlap or the value of the penalty term. Afterwards the total contact force is obtained by integrating the elementary forces defined in Eq. (6) over the overlapping area S as it is shown in Eq. (8).

$$\boldsymbol{f} = \int_{S=\beta_t \cap \beta_c} [grad\varphi_c - grad\varphi_t]\, dA\,, \tag{8}$$

This integral can be transformed into a line integral over the boundary of the overlapping area Γ:

$$\boldsymbol{f} = \oint_{\Gamma=\beta_t \cap \beta_c} \boldsymbol{n}_\Gamma \cdot (\varphi_c - \varphi_t)\, d\Gamma\,, \tag{9}$$

where $\boldsymbol{n}_\Gamma$ is the outward unit normal to the boundary of the overlapping area.

Since in the *FEM/DEM* individual discrete elements are discretized into finite elements, the previous integrals can be represented by the summation over finite elements as it is shown in Eq. (10) and Eq. (11).

$$\boldsymbol{f} = \sum_{i=1}^{n}\sum_{j=1}^{m}\int_{\beta_{t_j}\cap\beta_{c_i}} \left[grad\varphi_{c_i} - grad\varphi_{t_i}\right] dA\,. \tag{10}$$

$$\boldsymbol{f} = \sum_{i=1}^{n}\sum_{j=1}^{m}\int_{\Gamma=\beta_{t_j}\cap\beta_{c_i}} \boldsymbol{n}_{\Gamma=\beta_{t_j}\cap\beta_{c_i}} \left[\varphi_{c_i} - \varphi_{t_j}\right] d\Gamma. \tag{11}$$

Hence, the contact force between overlapping discrete elements can be calculated by a summation over the edges of corresponding finite elements that overlap.

We mention, that in 3D the integral over the overlapping volume must be performed as it is shown in Eq. (12).

$$\boldsymbol{f} = \sum_{i=1}^{n}\sum_{j=1}^{m}\int_{\beta_{t_j}\cap\beta_{c_i}} \left[grad\varphi_{c_i} - grad\varphi_{t_i}\right] dV\,. \tag{12}$$

By replacing integration over finite elements by equivalent integration over finite element boundaries, the following equation for contact fore is obtained:

$$\boldsymbol{f} = \sum_{i=1}^{n}\sum_{j=1}^{m}\int_{S=\beta_{t_j}\cap\beta_{c_i}} \boldsymbol{n}\left[\varphi_{c_i} - \varphi_{t_j}\right] dS\,. \tag{13}$$

Thus, the contact force between overlapping discrete elements is calculated by summation over the surfaces of corresponding finite elements that overlap, where $\boldsymbol{n}$ is the outward unit normal to the surface of the overlapping volume.

As a summary, it was shown that using contact interaction algorithm based on the *potential field-based penalty function method* has several advantages. It works with distributed contact forces, thus no artificial stress concentrations arises due to the contact, which would cause unrealistic fracturing behaviour. Furthermore, these algorithms satisfy the energy preservation which is an essential requirement in simulating physical behaviour properly. Due to this fact, the application of any kind of artificial damping is unnecessary. This *potential force concept* allows easy sliding between contact surfaces, and accurate representation of the physical contact conditions onto which friction, sliding, plasticity, surface roughness, wet-dry conditions, etc. can be incorporated following relatively simple rules of potential distribution over the finite element. This technique uses only the data supplied in the in-core database for contact free finite element analysis and it is easily linked to contact detection algorithm such as *Munjiza-NBS contact detection algorithm*. The algorithm does not require detection of boundary surfaces and the contact force is discretised with the same algorithm and the same piece of code, regardless of the shape of discrete elements thus, algorithmic complexities are greatly reduced. All of these reasons lead to fact that this type of contact processing is in general faster than alternative solutions. For further details we refer to the book (Munjiza, 2004, pp. 35-72).

DEFORMABILITY OF ELEMENTS

As from the basic idea of the *combined finite-discrete element method* follows, the continuum behaviour (i.e. the deformability) of discrete elements are described with the means of the *finite element method*. Each discrete element has its own finite element mesh which is able to follow the deformations of the discrete element. Furthermore, as it was shown earlier, the finite element discretization of individual discrete elements describes the contact conditions between discrete elements due to the discretization of the distributed contact forces.

To describe the deformations of discrete elements, the classical equations and tensors of the continuum mechanics are used. Therefore, the current coordinates $\boldsymbol{x}$ of material points having reference position vector $\boldsymbol{p}$ can be written as:

$$\boldsymbol{x} = \boldsymbol{p} + \boldsymbol{u}(\boldsymbol{p}), \tag{14}$$

where $\boldsymbol{u}(\boldsymbol{p})$ is the displacement of material point. Deformations are described with the help of a strain tensor calculated from the *deformation gradient tensor* $\boldsymbol{F}(\boldsymbol{p})$:

$$\boldsymbol{F}(\boldsymbol{p}) = \nabla \boldsymbol{x} = \boldsymbol{I} + \nabla \mathbf{u}\,. \tag{15}$$

Typically, in a *FEM/DEM* simulation the well known strain measures of continuum mechanics for instance, the *right-* and *left Cauchy-Green*, *Green-St. Venant*, *Almansi-Hamel strain tensors*, *etc.* are used. Although in most cases it is enough to consider small strains, it is very important to note that in *FEM/DEM* simulations large displacements must be followed. In such a case when the stretches are small but the rotations and displacements are large it is practical to decompose the deformation gradient tensor in the following way:

$$\boldsymbol{F} = \boldsymbol{R}\boldsymbol{U} = \boldsymbol{V}\boldsymbol{R}\,, \tag{16}$$

where $\boldsymbol{U}$ is the right stretch tensor, $\boldsymbol{V}$ is the left stretch tensor and $\boldsymbol{R}$ is the orthogonal rotation tensor. Following the polar decomposition of the deformation gradient tensor, the right Green-St. Venant strain tensor $\overline{\boldsymbol{E}}$ can be expressed as:

$$\overline{\boldsymbol{E}} = \frac{1}{2}\left(\boldsymbol{U}^{\boldsymbol{T}}\boldsymbol{U} - \boldsymbol{I}\right). \tag{17}$$

The application of $\boldsymbol{U}$ right stretch tensor physically means that the material is first stretched in the principal directions and it is followed by the rotation. The reverse procedure can be performed by using the left stretch tensor $\boldsymbol{V}$. Here the left Green-St. Venant strain tensor is applied as:

$$\widetilde{\boldsymbol{E}} = \frac{1}{2}\left(\boldsymbol{V}\boldsymbol{V}^{\boldsymbol{T}} - \boldsymbol{I}\right). \tag{18}$$

In this case, the rotation occurs first, then the stretches already occur in the principal directions of the rotated configuration.

In order to measure the stress variables the *Cauchy*, *First- or Second Piola-Kirchhoff stress tensors* can be applied. In the calculations some kinds of constitutive relations are applied which make connection between stresses and strains and contain failure criteria. Discussion of further details about the typical steps of continuum mechanics is out of the scope of this chapter. Additional details can be found for instance, in (Munjiza, 2004, pp. 131-177) and (Belytschko, Liu, & Moran, 2000, pp. 75-137).

Since the finite element discretization is also used to process contact interaction, in general, it is important to employ as simple geometry of finite elements as possible in order to obtain efficient contact interaction algorithm. Due to this fact, mainly constant strain triangle finite elements are used in 2D and constant strain tetrahedron elements are used in case of 3D analyses. However in case of relatively incompressible solids, locking problems are associated with these linear finite elements which can seriously degrade the accuracy of the simulations. Therefore, in the paper (Xiang, Munjiza, & Latham, 2009), finite strain, finite rotation quadratic tetrahedral elements were implemented into the *FEM/DEM*.

FRACTURE AND FRAGMENTATION ALGORITHMS

The appropriate modelling of transition from continua to discontinua processes including fracture and fragmentation plays an essential role in a *FEM/DEM* analysis. In order to describe these phenomena so-called fracture and fragmentation algorithms are used which handle the creation of new boundaries and new discrete elements under certain loading conditions.

A fracture and fragmentation algorithm is responsible to solve several tasks. Namely, it has to describe the conditions under crack initiation appears, and the way how it propagates. During the crack propagation remeshing is necessary, thus variables must be transformed from the old mesh to the new one. Additionally, released internal forces must be replaced with equivalent contact forces.

Several different approaches exist how to perform the analysis of cracks. The global approach is based on the representation of the stress singularity at the crack tip. This singularity can be characterized by the energy release rate G_f. However local approaches usually apply a smeared crack approach, where the crack is replaced by a blunt crack band and the crack propagation processes are described with the help of constitutive laws or formulations of damage mechanics. Furthermore, the single crack approach considers a plastic zone at the crack tip, and the plastically strained material is replaced by a zone of weakened bonds between the crack walls. In the *combined finite-discrete element method* a fracture based softening plasticity framework is applied, where the energy dissipation is considered through a mesh size dependent softening modulus as it is detailed in (Munjiza, Owen, & Bicanic, 1995). After further research (Munjiza, Andrews, & White, 1999) the combination of smeared and single crack approaches was implemented. The aim of this coupling was to model multiple-crack, and progressive fracture situations. In this *combined single and smeared crack model* the strain-hardening part of the stress-strain curve is considered through constitutive laws, while the strain-softening part is treated by the softening stress-displacement relationship being implemented through the single crack model as it can be seen in Figure (4). In this approach, the plastic zone is represented by bonding stress being the function of crack opening.

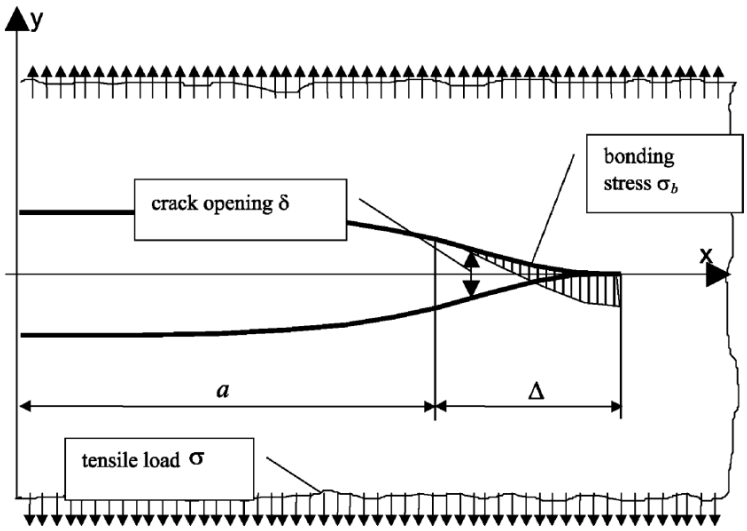

Figure 4 Plastic zone represented by bonding stress being a function of crack opening
Source: Munjiza & John, 2002

The separation begins when bonding stress σ_b is equal to the tensile strength f_t. With increasing separation $\delta > \delta_t$ the bonding stress decreases and at separation $\delta = \delta_c$ the bonding stress drops to zero. The value of bonding stress for separation $\delta_t < \delta < \delta_c$ is given by

$$\sigma_b = z f_t \,, \tag{19}$$

where z is the scaling (softening) function given by

$$z = \left[1 - \frac{a+b-1}{a+b} exp\left(D \frac{a+cb}{(a+b)(1-a-b)}\right)\right][a(1-D) + b(1-D)^c] \,, \tag{20}$$

where the variable D is given by

$$D = \begin{cases} 0 & \text{if } \delta \leq \delta_t \\ 1 & \text{if } \delta > \delta_c \\ \dfrac{\delta - \delta_t}{\delta_c - \delta_t} & \text{otherwise} \end{cases} . \tag{21}$$

Using Eq. (20) for the determination of scaling (softening) function z, the bonding stress will approximate the experimental stress-displacement curve, while the parameters a, b and c are obtained by curve fitting (Munjiza, Andrews, & White, 1999). In FDEM the joint element acts as a bond between edges of two triangular finite elements. These bond represents the fracture mechanism termed as a *combined single and smeared crack model* (Munjiza, Andrews, & White, 1999).

Due to the finite element discretization of the governing equations, an approximated stress and strain field near the crack tip can be obtained. It was shown in (Munjiza, Andrews, & White, 1999), that in order the get accurate results a very fine mesh is required near the crack tip, namely the size of the finite elements must be much smaller than the actual size of the plastic zone. It is important to note, that the *combined single and smeared fracture algorithm* is sensitive to the size of the finite elements situated in vicinity of the crack tip. In case of a very fine mesh, accurate results can be obtained, but if a very coarse mesh is applied, then the calculated failure load tends to the failure load belonging to the uniform stress distribution, and even in case of applying intermediate size of elements, the obtained

critical load will be overestimated. Beside the enormous computational challenge caused by contact detection, contact interaction algorithms, and time integration, the fracture and fragmentation algorithms provides a huge computational task additionally, which – at least nowadays - may restrict the application of the *combined finite-discrete element method* in case of large-scale engineering problems.

TIME INTEGRATION

In order to reduce the CPU time, explicit time integration schemes may be applied. As it was mentioned earlier, the so-called lumped mass matrix approach is used, thus diagonal mass matrix is considered during the analysis. Furthermore, the assembling of stiffness matrix can also be avoided by using an explicit time integration scheme. Traditionally, the central difference method has been employed to solve the equation of motion. Since it is a conditionally stable technique, the stability and the required accuracy are achieved through reducing the size of the time step. As an alternative technique the *Gear's predictor-corrector time integration schemes* should be mentioned. These schemes always includes three stages, namely:

- Prediction stage, where the positions of the elements are calculated at $t + \Delta t$ using Taylor series based on positions and their time derivatives.
- Evaluation stage, where the forces f_{t+h} are evaluated based on the position of the elements calculated in the prediction stage. From this force, the accelerations at $t + \Delta t$ can be calculated, and difference can be determined between the predicted and the calculated accelerations.
- Correction stage, where the predicted positions and its time derivatives are corrected using the discrepancy between accelerations calculated in the evaluation stage.

It should be mentioned that in the book (Munjiza, 2004, pp. 203-208) further alternative explicit time integration techniques, for instance *CHIN,OMF30* and *OMF32* integration schemes are detailed. All of these techniques can be used in a *FEM/DEM* simulation. The decision about which scheme should be used depends on their efficiency in terms of stability, accuracy and CPU time. In the book (Munjiza, 2004, pp. 208-211), a comparison analysis can be found for a single degree of freedom system. It was shown that although in some cases the higher order methods work with larger values of critical time steps, still the higher order methods not necessarily faster than lower order schemes. This conclusion is especially true in case of large scale systems, where contact detection, contact interaction, fracture and fragmentation may be involved, and higher order schemes require multiple force evaluation which is much less efficient than lower order methods.

PARALLELIZATION

As it has been mentioned, the limitation of *FEM/DEM* is that it is CPU-intensive, thus it is difficult to analyze large scale problems on sequential CPU hardware. Therefore, researches (Owen, Feng, Han, & Peric, 2000), (Owen & Feng, 2001), (Wang, Feng, & Owen, 2004)] were carried out in order to implement the possibility to use high-performance parallel computers. In all those studies, a master/slave approach was adopted meaning that one master processor was performing domain decomposition and load balancing tasks, then distributing work to slave processors. Some general strategies for parallelization of *FEM/DEM* are described in (Munjiza, Knight, & Rougier, 2012). Later, other versions appeared as static domain decomposition (Schiava D'Albano, 2014), hardware independent *FEM/DEM* parallelization framework by using virtual parallel machine (Lei, Rougier, Knight, & Munjiza, 2014), and dynamic domain decomposition based parallelization where all tasks (domain decomposition, load balancing) are performed concurrently on all processors (Lukas, Schiava

D'Albano, & Munjiza, 2014). Parallelization strategies usually attempt to divide the large problem (computational domain) into a number of smaller sub-problems (sub-domains). A good parallel implementation has to fulfil two - often competing - requirements, namely each processor must be kept busy doing useful work and the communication between processors must be kept to a minimum. Today, parallelization algorithms are available in *FEM/DEM* codes, thus - at least in many cases - the solution of large scale problems became possible.

EXAMPLES FOR COMBINED FINITE-DISCRETE ELEMENT SIMULATIONS

In the following, some examples are mentioned for the application of the *combined finite-discrete element method.* This part focuses on the modelling of masonry structures, however other applications are shortly mentioned as well.

Firstly, referring to the paper (Nikolic, Smoljanovic, & Zivaljic, 2013), seismic analysis of dry stone masonry structures were performed with the help of the *FEM/DEM*. In this work each stone block was modelled as a discrete element which was discretized by constant strain triangular finite elements. The fracture and fragmentation processes were considered through contact elements which were implemented within the finite element mesh. In the applied *FEM/DEM* code the *Munjiza-NBS contact detection algorithm* was implemented. In the contact interaction algorithm the *potential contact force concept was applied* and the *Coulomb-type condition* was used to analyze the friction between discrete elements. The cracks were assumed to coincide with the finite element edges and the separation of these edges induced a bonding stress which was taken to be a function of the size of the separation. At first, numerical calculations for the analysis of shear behaviour of stone masonry joints were performed. Two different pre-compression stresses were applied and after shear tests were carried out under displacement control and the numerical results showed a great correspondence with the experimental results. Afterwards the behaviour of existing structures were analysed under seismic effects. The dynamic response of the structure of the *Prothyron* - which is a certain part of *Diocletian's Palace* in Split - was simulated with the *combined finite-discrete element method*. The *FEM/DEM* model of the structure can be seen in Figure (5).

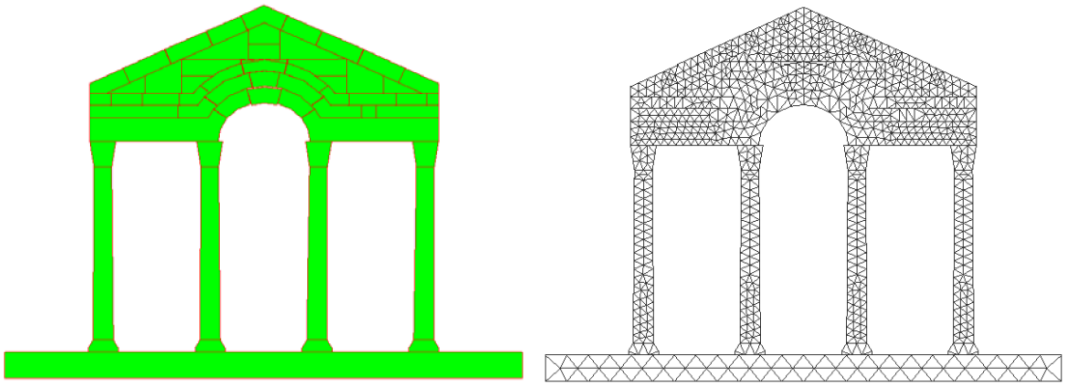

Figure 5 FEM/DEM model of Prothyron including discrete elements (left) and FEM mesh (right) Source: Nikolic, Smoljanovic, & Zivaljic, 2013

The structure was subjected to gradually increasing horizontal ground acceleration until the collapse occurred. The collapse process of the structure can be seen in Figure (6).

Figure 6 Collapse simulation of Prothyron due to seismic effect using FEM/DEM
Source: Nikolic, Smoljanovic, & Zivaljic, 2013

This research (Nikolic, Smoljanovic, & Zivaljic, 2013) showed the advantage of using the *combined finite-discrete element method* - which derives from the possibility of modelling the fragmentation of blocks - for analysis of failure modes of structures under hazardous loads. The results of the performed analyses showed good agreement with the experiments, thus this paper demonstrates the potential of the *FEM/DEM* for realistic modelling of the response of dry masonry structures. Further details can be found in the original paper (Nikolic, Smoljanovic, & Zivaljic, 2013).

In paper (Smoljanovic, Zivaljic, & Nikolic, 2013) the authors analyzed the behaviour of a dry stone masonry bell tower exposed to impact and seismic load. Again the whole structural failure (transition from continua to discontinua) process due to impact load was simulated as it is shown in Figure (7).

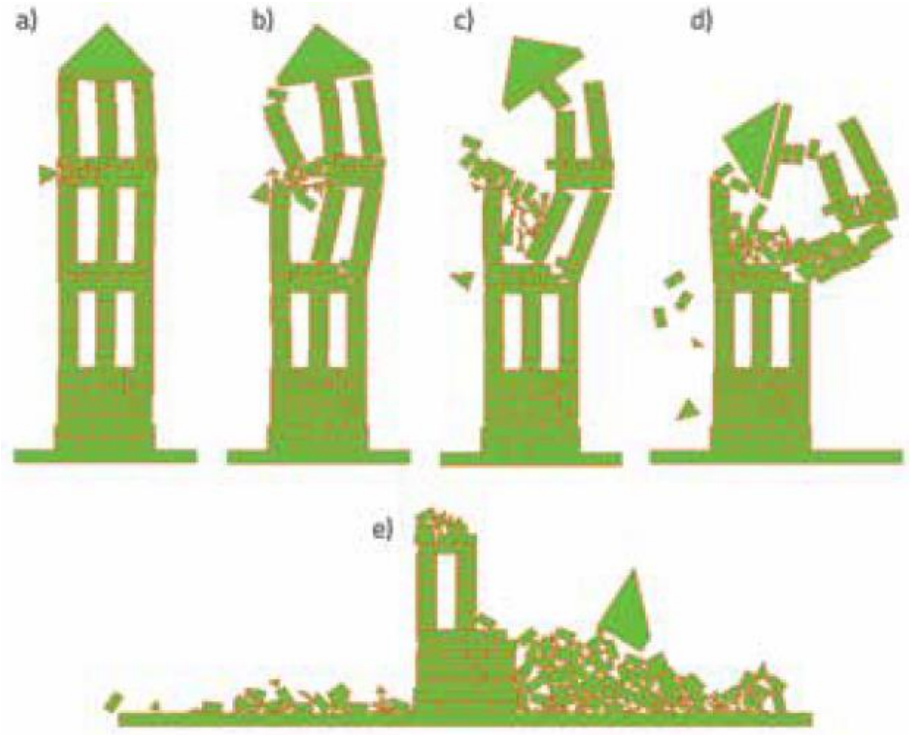

Figure 7 Collapse simulation of dry stone masonry bell tower exposed to projectile impact using FEM/DEM. Source: Smoljanovic, Zivaljic, & Nikolic, 2013

Using the *combined finite-discrete element method* the detailed analysis of failure was carried out including energy dissipation during the impact, initiation and propagation of cracks and the inertia effect of the individual parts of the structure. The seismic analysis of the structure was also performed

which enables the determination of the load bearing capacity and the behaviour factor of the structure. The collapse simulation under seismic effects can be seen in Figure (8).

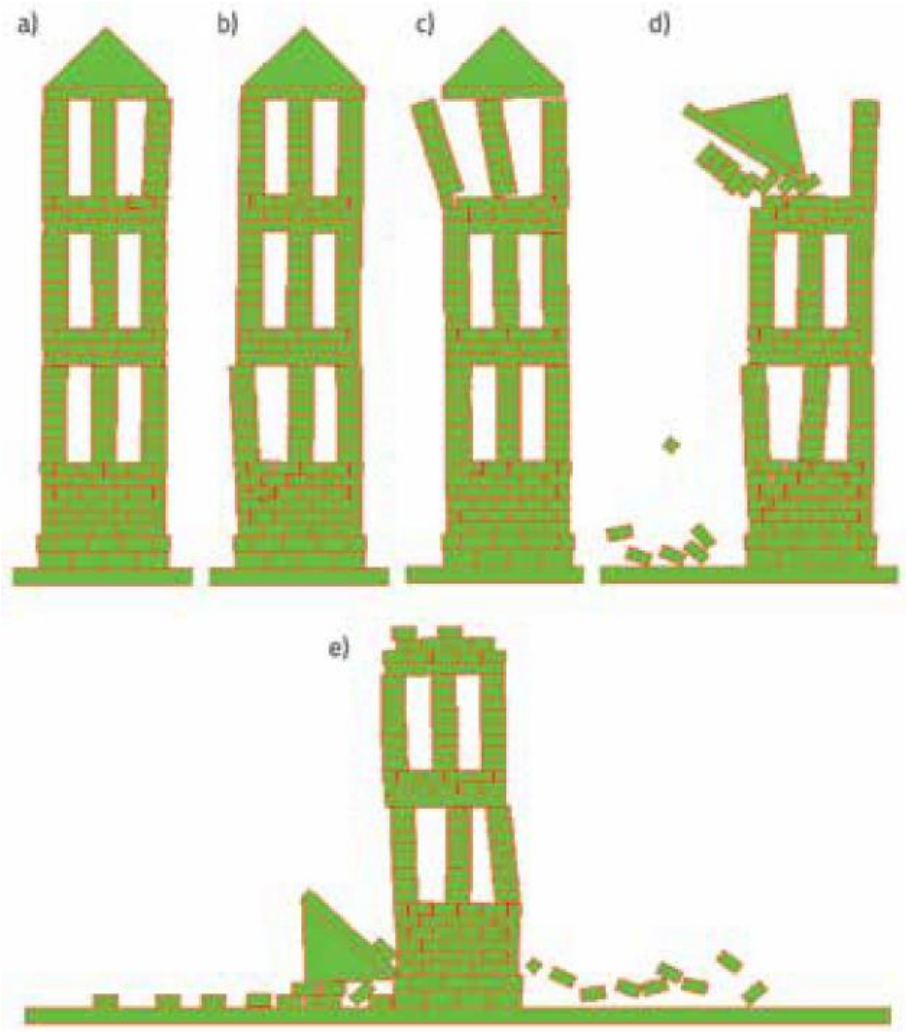

Figure 8 Collapse simulation of dry stone masonry bell tower exposed to seismic effects using FEM/DEM. Source: Smoljanovic, Zivaljic, & Nikolic, 2013

In the paper (Smoljanovic, Zivaljic, & Nikolic, 2013) the advantage of the *combined finite-discrete element method* in performing collapse simulations were shown. The applied numerical model was able to simulate the whole structural failure process including large displacements and rotations of stone blocks subjected to friction force acting between them. Further details of the analyses can be found in the original paper (Smoljanovic, Zivaljic, & Nikolic, 2013) including numerical analyses of reinforced concrete structures as well.

In the paper (Baraldi, Reccia, Cazzani, & Cecchi, 2013) a comparative study is discussed. Discrete models and *FEM/DEM* models were used to investigate the in-plane behaviour of periodic brickwork. In the *FEM/DEM* simulations elastic blocks were considered by means of finite elements, but on the other hand, rigid discrete elements were applied in the discrete model. In the *FEM/DEM* model the mortar joints were idealized as elastic or elasto-plastic zero-thickness *Mohr-Coulomb* interfaces. Two different joint types were applied in the *FEM/DEM* simulations. One of these was implemented inside the block and this worked with a high cohesion value in order to avoid the breaking of blocks, however a much smaller cohesion value was applied for joints placed between the blocks in order to model the separation of blocks along the mortar joints. In this paper (Baraldi, Reccia, Cazzani, &

Cecchi, 2013) masonry panels were subjected to in plane actions, like compression and shear forces in horizontal and vertical directions. Some deformed shapes of the *FEM/DEM* and discrete models due to horizontal shear effects can be seen in Figure (9).

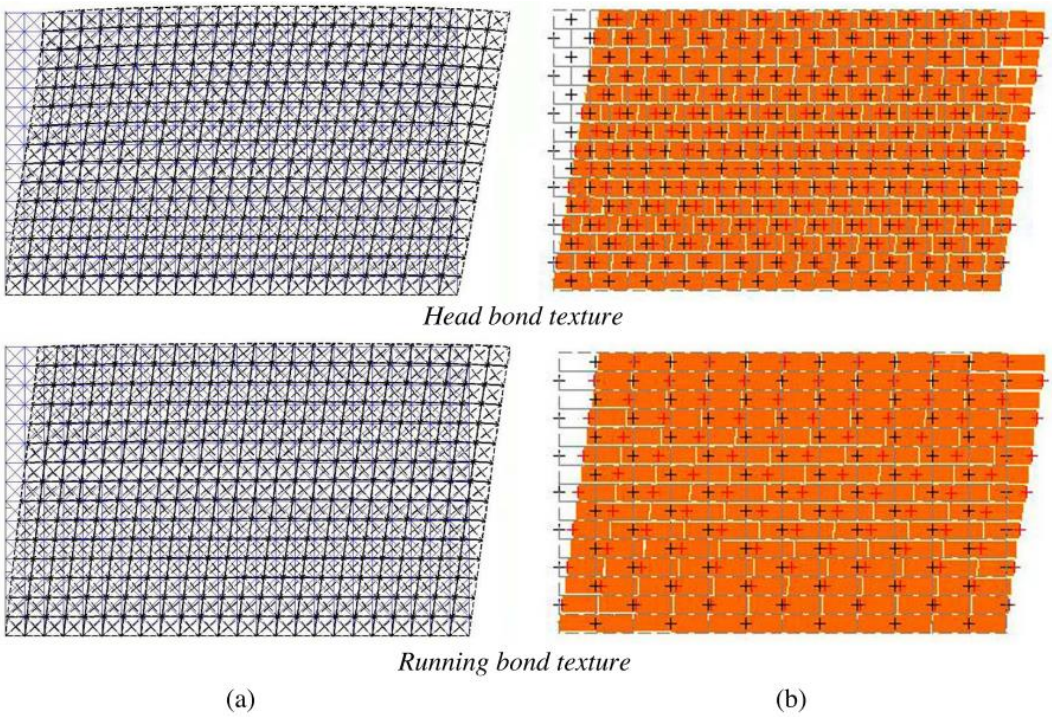

Figure 9 Horizontal shear deformed mesh: (a) FEM/DEM model; (b) Discrete model
Source: Baraldi, Reccia, Cazzani, & Cecchi, 2013

The authors of paper (Baraldi, Reccia, Cazzani, & Cecchi, 2013) found that in case of vertical and horizontal compressive forces applied, models show a very good agreement in terms of displacements and reactions. In case of compression, the influence of the texture pattern in the *FEM/DEM* model is less evident than in the discrete model due to the elastic behaviour of mortar joints. Even in case of horizontal shear force the two models were in very good agreement for the running bond pattern, however significant differences occurred for the head bond pattern. In case of vertical shear force the two models were in excellent agreement for both the texture patterns considered. Further details can be found in the paper (Baraldi, Reccia, Cazzani, & Cecchi, 2013).

In the paper (Owen, Peric, Petrinic, Smokes, & James, ?) masonry arch bridge with backfill and masonry arch bridge with anchor stitching system were analysed with the *combined finite-discrete element method*. The complex problem including masonry units, granular back-fill and geotechnical foundation material was considered. Here the masonry blocks were represented by deformable discrete elements in frictional contact. The fill material was modelled by spherical discrete elements, however the foundation medium was considered as a *Mohr-Coulomb* material. In case of the strengthened bridge the anchor system was modelled as an elasto-plastic steel bar, and the grouted bond with the masonry was simulated by prescribing a nonlinear shear stress/strain relation, whose parameters were determined from laboratory anchor pull-out tests. The *FEM/DEM* discretization and the deformations of the strengthened bridge just before the bottom ring fell away can be seen in Figure (10). Further information about the performed analyses can be found in the paper (Owen, Peric, Petrinic, Smokes, & James, ?).

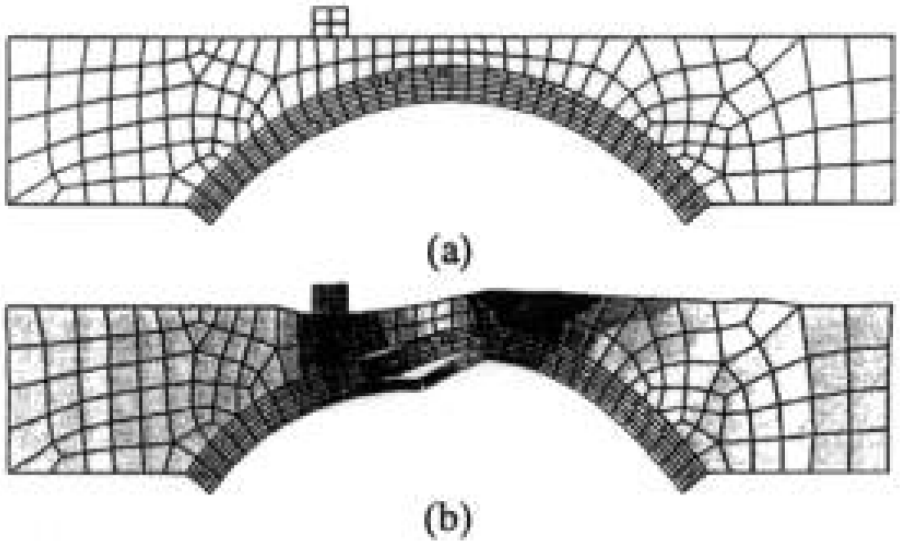

Figure 10 FEM/DEM discretization of masonry arch bridge (a); Deformations just before the collapse. Source: (Owen, Peric, Petrinic, Smokes, & James, ?)

Apart from the numerical simulations of structures the *combined finite-discrete element method* proved to be a very effective tool in case of biomechanical applications as well. We refer for instance, to the paper (Xu et al., 2013), where large scale simulations of red blood cell aggregation in shear flows were performed with the help of *FEM/DEM*.

CONCLUSION

In this chapter the main characteristics and steps of the *combined finite-discrete element method* were discussed. The specific contact detection, contact interaction, fracture and fragmentation algorithms were mentioned, which are typically used in *FDEM* simulations. Furthermore, the huge computational challenge in case of large scale problems were pointed out, and the time stepping process with certain parallelization techniques were shortly mentioned. Examples were collected from the literature, where the authors proved the efficiency of the *combined finite-discrete element method* in the appropriate modelling of masonry structures.

ADDITIONAL READINGS

As a final remark, for the interested readers, the presence of open source *combined finite-discrete element* codes, Y2D and Y3D should be mentioned. These codes include the above mentioned algorithms and have already served as a basic tool in case of several *FEM/DEM* researches. Additionally, Y-GUI graphical user interface is available (Mahabadi, Grasselli, & Munjiza, 2010), which provides the possibility to set up models graphically, instead typing the entire input file in ASCII text editor, significantly reducing the time needed to create the geometry of the model. Further information can be found on the following website: http://vgest.net/.

REFERENCES

Baraldi, D., Reccia, E., Cazzani, A., & Cecchi, A. (2013) *Discrete and finite element models for periodic brickwork: a comparative analysis*. Paper presented at AIMETA, Torino, Italy.

Belytschko, T., Liu, W. K., & Moran, B. (2000) *Nonlinear finite elements for continua and structures.* John Wiley & Sons Ltd.

Lei, Z., Rougier, E., Knight, E.E., & Munjiza, A. (2014). A framework for grand scale parallelization of the combined finite discrete element method in 2D. *Computational Particle Mechanics, 1(3),* 307-19.

Lukas, T., Schiava D'Albano, G.G., & Munjiza, A. (2014). Space decomposition based parallelization solutions for the combined finite-discrete element method in 2D. *Journal of Rock Mechanics and Geotechnical Engineering, 6,* 607-615.

Mahabadi, O.K., Grasselli, G., & Munjiza, A. (2010). A graphical user interface and pre-processor for the combined finite-discrete element code, Y2D, incorporating material heterogeneity. *Computers & Geosciences, 36,* 241-252.

Munjiza, A. (2004). *The combined finite-discrete element method*. John Wiley & Sons Ltd.

Munjiza, A., & Andrews, K.R.F. (2000). Penalty function method for combined finite-discrete element systems comprising large number of separate bodies. *International Journal for Numerical Methods in Engineering, 49,* 1377-1396.

Munjiza, A., Andrews, K.R.F., & White, J.K. (1999). Combined single and smeared crack model in combined finite-discrete element method. *International Journal for Numerical Methods in Engineering, 44,* 41-57.

Munjiza, A., & John, N.W.M. (2002). Mesh size sensitivity of the combined FEM/DEM fracture and fragmentation algorithms. *Engineering Fracture Mechanics, 69,* 281-295.

Munjiza, A., Knight, E.E., & Rougier, E. (2012). *Computational mechanics of discontinua*. Chichester, UK: John Wiley & Sons.

Munjiza, A., Rougier, E., & John, N.W.M. (2006). MR linear contact detection algorithm. *International Journal for Numerical Methods in Engineering, 66(1).*

Munjiza, A., Owen, D.R.J., & Bicanic, N. (1995). A combined finite discrete element method in transient dynamics of fracturing solids. *Engineering Computations, 12(2),* 145-74.

Nikolic, Z., Smoljanovic, H., & Zivaljic, N. (2013). A combined finite-discrete element analysis of dry stone masonry structures. *Engineering Structures, 52,* 89-100.

Owen, D.R.J., & Feng, Y.T. (2001). Parallelised finite/discrete element simulation of multi-fracturing solids and discrete systems. *Engineering Computations 18(3-4),* 557-76.

Owen, D.R.J., Feng, Y.T., Han, K., & Peric, D. (2000). *Dynamic domain decomposition and load balancing in parallel simulation of finite/discrete elements.* Paper presented at European Congress on Computational Methods in Applied Sciences and Engineering, Barcelona, Spain.

Owen, D.RJ., Peric, D., Petrinic, N., Smokes, CL., & James, P.J. (?). Finite/discrete element models for assessment and repair of masonry structures, ?

Schiava D'Albano, G.G. (2014). *Computational and algorithmic solutions for large scale combined finite-discrete elements simulations.* (Unpublished? doctoral dissertation). London, UK: Queen Mary, University of London.

Schiava D'Albano, G.G., Munjiza, A., & Lukas, T. (2013). *Novel MS (MunjizaSchiava) contact detection algorithm for multi-core architectures.* Paper presented at Particles, Stuttgart, Germany.

Smoljanovic, H., Zivaljic, N., & Nikolic, Z. (2013). Nonlinear analysis of engineering structures by combined finite-discrete element method. *Gradevinar, 65,* 331-334.

Wang, F., Feng, Y.T., & Owen, D.R.J. (2004). Parallelization for finite-discrete element analysis in a distributed-memory environment. *International Journal of Computational Engineering Science, 5(1),* 1-23.

Xiang, J., Munjiza, A., & Latham, J.-P. (2009). Finite strain, finite rotation quadratic tetrahedral element for the combined finite-discrete element method. *International Journal for Numerical Methods in Engineering, 79(8),* 946-978.

Xu, D., Kaliviotis, E., Munjiza, A., Avital, E., Ji, C., & Williams, J. (2013). Large scale simulation of red blood cell aggregation in shear flows. *Journal of Biomechanics, 46,* 1810-1817.